Nanoscale Res Lett (2007) 2:1–5
DOI 10.1007/s11671-006-9020-x

NANO EXPRESS

A solution blending route to ethylene propylene diene terpolymer/layered double hydroxide nanocomposites

H. Acharya · S. K. Srivastava · Anil K. Bhowmick

Published online: 27 October 2006

Abstract Ethylene propylene diene terpolymer (EPDM)/MgAl layered double hydroxide (LDH) nanocomposites have been synthesized by solution intercalation using organically modified LDH (DS-LDH). The molecular level dispersion of LDH nanolayers has been verified by the disappearance of basal XRD peak of DS-LDH in the composites. The internal structures, of the nanocomposite with the dispersion nature of LDH particles in EPDM matrix have been studied by TEM and AFM. Thermogravimetric analysis (TGA) shows thermal stability of nanocomposites improved by ≈40 °C when 10% weight loss was selected as point of comparison. The degradation for pure EPDM is faster above 380 °C while in case of its nanocomposites, it is much slower.

Keywords Layered double hydroxide · Nanocomposites · Solution blending

Introduction

The recent research in polymer nanocomposite is focused on the use of layered double hydroxide as inorganic layered crystal for their wide application in catalysis, hydrogenation reaction, fire retardance, stabilizer, medical applications, sorbent and ion exchangers [1, 2]. These nanocomposites can be considered to be reinforced by the nanofiller and follow the various unique properties such as enhanced mechanical properties, thermal stability, improved gas barrier properties and reduced flammability [3–8]. The LDH has an ideal formula of $[M^{II}_{(1-x)}M^{III}_{x}(OH)_2]^{x+}A^{m-}_{x/m} \cdot nH_2O$, where M^{II} is divalent metal ion, M^{III} is trivalent metal ion and A is an exchangeable interlayer anion [2]. In LDH, the hydroxide sheets stacked with strong interaction due to high intergallery charge density [9]. Pure inorganic LDH is incompatible with the organic non-polar polymer chains and also the interlayer spacing between the metal hydroxide layers (0.76 nm) is not suitable for large polymer chain intercalation [10, 11]. Therefore, the organic anions are intercalated in the interlayer space of LDH to make it organophilic, which weaken the electrostatic forces operating between the hydroxide sheets. In past, few reports were published on EPDM/layered silicate nanocomposites [12, 13] but to the best of our knowledge, there is no work reported so far on ethylene propylene diene terpolymer (EPDM)/MgAl layered double hydroxide (LDH) nanocomposites. The present work reports the synthesis and characterization of exfoliated EPDM/LDH nanocomposites by solution intercalation method. Inorganic LDH was made organophilic by the intercalation of dodecyl sulfate (DS) anion in the interlayer. Characterization focused on the morphology and thermal stability of nanocomposites.

Experimental

The two dimensional Mg/Al LDH precursor was prepared following a standard co-precipitation and

H. Acharya · S. K. Srivastava (✉)
Department of Chemistry, Indian Institute of Technology, Kharagpur, West Bengal 721302, India
e-mail: sunit@chem.iitkgp.ernet.in

A. K. Bhowmick
Rubber Technology Centre, Indian Institute of Technology, Kharagpur 721302, India

thermal crystallization method of mixed metal ions with base from aqueous solution. In a typical preparation, 100 ml aqueous solution of a stoichiometric amount of $Mg(NO_3)_2 \cdot 6H_2O$ (0.075 mol, Merck, India) and $Al(NO_3)_3 \cdot 9H_2O$ (0.025 mol, Merck, India) was slowly added into 100 ml of NaOH (0.2 mol, S. D. fine-chemicals, Boisar) and Na_2CO_3 (0.025 mol, Merck, India) aqueous solution. The solution pH was adjusted to 9 ± 1 with 1 mol/L of NaOH. The resulting white precipitate was then aged at 70 °C for 24 h, filtered, washed and dried. The organophilic LDH was prepared by the rehydration process of calcined MgAl-LDH. For this, 2.5 g of MgAl-LDH was calcined at 500 °C for 5 h, and then suspended in a 120 ml of aqueous solution containing 2.5 g of sodium dodecyl sulphate (SDS, SRL Pvt., Ltd., India) under refluxing condition for 12 h to yield a white powder DS-LDH. Ethylene propylene diene terpolymer (EPDM, Keltan 520, density 0.86 g/mL, ethylene content 58 wt%) was received from DSM, Netherlands. The EPDM nanocomposites with different wt% of DS-LDH were prepared by the solution intercalation method. Firstly, the desired amount of DS-LDH in 50 ml of toluene was dispersed for 5 h. Subsequently this solution was added to the EPDM solution in toluene and refluxed for another 12 h. Finally the dicumyl peroxide (DCP, 98%, Hercules, Inc. United States) was added as catalyst for cross-linking purpose and afterwards solvent was extracted under reduced pressure. The resultant composites were compression molded by a hydraulically operated press at 150 °C for 45 min. The preparation conditions were same for each composition and they were designated as ELn (where, n represents the wt% of DS-LDH content).

Results and discussion

X-ray diffraction studies of LDH, EPDM and their nanocomposites were performed with a Rigaku Miniflex diffractometer using Cu Kα radiation. Figure 1 shows the XRD pattern in the range of 2θ = 10–70° for MgAl-LDH as a pure hydrotalcite. The diffraction peaks of the MgAl-LDH have been indexed according to the JCPDS X-ray diffraction file (No. 22-700). The basal diffraction peak is the 003 diffraction peaks which corresponds to the basal spacing of 0.77 nm, close to the value of 0.78 nm reported by Chibwe and Jones [14]. Figure 2a and 2b shows the XRD pattern of DS-LDH and EPDM/DS-LDH in the angle range of 2–15° and 15–70°, respectively. These patterns show the structural changes of the samples with the loading of DS-LDH. It shows the basal spacing for the DS-LDH

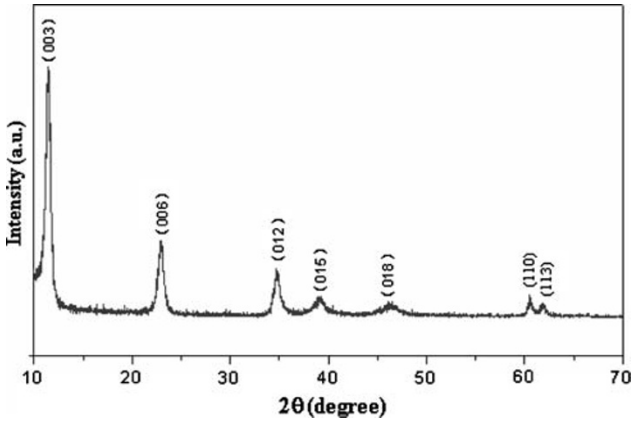

Fig. 1 XRD pattern of Mg/Al LDH

is 2.56 nm from the diffraction peak at 2θ = 3.45°. The individual dodecyl sulphate chain length and LDH sheet thickness are 2.07 and 0.48 nm, respectively [15, 16]. As a result, the increase in basal spacing is due to the intercalation of mono-layer dodecyl sulphate molecules between the hydrotalcite sheets. However, XRD patterns of EPDM/LDH nanocomposites in Fig. 2a and 2b do not exhibit any peak corresponding to the DS-LDH, which indicates that the organically modified MgAl-LDH layers are exfoliated in the EPDM matrix.

Fourier Transform Infrared (FTIR) analysis was performed and the spectra were recorded using a Thermonicolet/Nexus 870 FTIR spectrometer and displayed in Figs. 3 and 4. The pure MgAl-LDH and DS-LDH shows a broad band in the range of 3400–3500 cm^{-1} corresponding to the OH stretching frequency. The peak at around 1380 cm^{-1} is due to the stretching mode of the carbonate molecules. The stretching band for aliphatic CH_3– or-CH_2– of long chain DS molecules appears at around 2850–2960 cm^{-1}. The peak at 1470 cm^{-1} is due to the deformation vibration of –CH_2- and –CH_3. The band at 1220 cm^{-1} and 1247 cm^{-1} represents the stretching vibration of sulfate in DS-LDH. These peaks demonstrated that DS was intercalated into the LDH. The bands recorded in the low frequency region of 800–400 cm^{-1} are attributed to the M–O and O–M–O (M = Mg or Al) vibration of metal-oxygen bond in the brucite-like lattice [17]. The FTIR spectra of EPDM/LDH nanocomposite with compare to the pure EPDM in Fig. 4 shows some new peaks in the region of 1640 cm^{-1} for H–OH vibration. The peaks at around 640 cm^{-1}, 590 cm^{-1} and 410 cm^{-1} are assigned to Mg–O, Al–O stretching vibration mode and O–M–O lattice vibration, respectively. This indicates the presence of layered double hydroxide in the EPDM matrix.

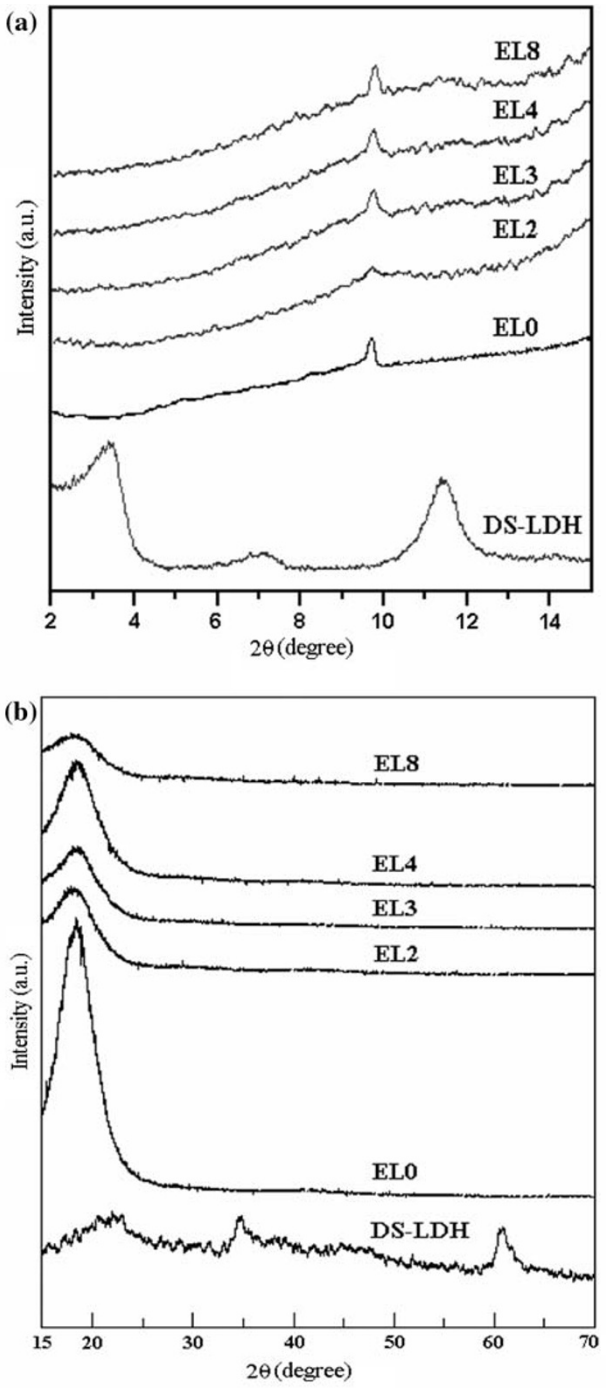

Fig. 2 XRD spectra of EPDM/LDH composites with varying LDH contents at (**a**) lower angle range (**b**) higher angle range

Figure 5 shows the TEM images of EPDM/DS-LDH nanocomposite using JEM-2000 FX II -JEOL transmission electron microscope. The distribution of the LDH particles in the EPDM matrix appears to be inhomogeneous as shown in Fig. 5a. However, TEM micrograph at higher magnification in Fig. 5b shows the exfoliated dispersion of LDH particles with average thickness of 50–100 nm and length of 2–4 nm within the EPDM matrix. The TEM images in Fig. 5c clearly demonstrate the detachment and molecular level dispersion of the tiny clusters from the surface of the LDH particle into the EPDM matrix.

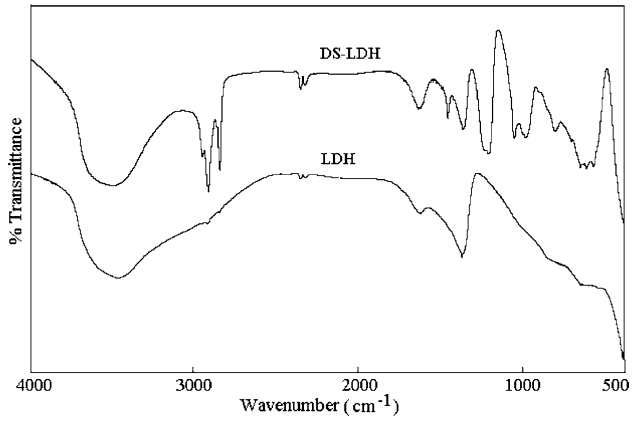

Fig. 3 FTIR spectra of LDH and DS-LDH

The internal structure of nanocomposite, with the emphasis on the dispersion nature of DS-LDH particles in EPDM matrix can observed directly by using a Nanoscope IIIa atomic force microscopy (AFM). Figure 6 shows the phase contrast image of EPDM/LDH nanocomposite, which indicates sufficient intrinsic contrast between the inorganic LDH particles and the EPDM matrix. It is evident from the image that the LDH particles are well dispersed in the nanocomposite EPDM matrix. The apparent broadening feature of height in the LDH particle distribution is possibly due to the interaction of the tip with submerged LDH platelets in nanocomposite, which are not perfectly

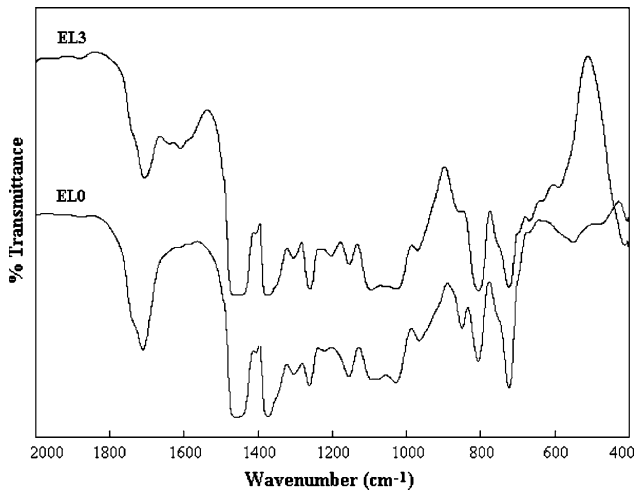

Fig. 4 FTIR spectra of pure EPDM and EPDM/DS-LDH nanocomposite

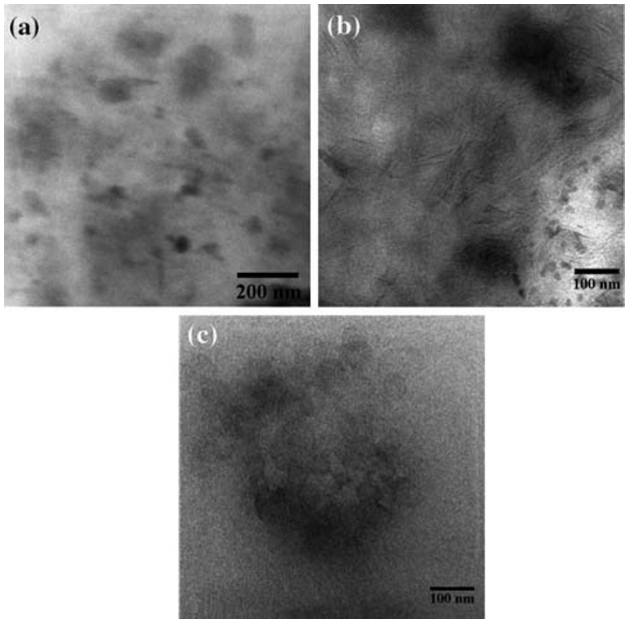

Fig. 5 TEM images of EPDM/DS-LDH nanocomposite showing (**a**) at low magnification, (**b**) at high magnification, (**c**) molecular level LDH platelet dispersion

perpendicular to the EPDM matrix. These observations are also in accordance with the TEM studies as discussed earlier.

Thermogravimetric analysis of pure EPDM and its corresponding nanocomposites with DS-LDH were perfomed in an air atmosphere on a Perkin Elmer thermal analyzer with a heating rate of 20 °C/min over a temperature sweep from 50 °C to 600 °C and are displayed in Fig. 7. It shows that the EPDM/DS-LDH nanocomposites have much higher degradation temperature than the neat EPDM. The degradation corresponding to the main chain scission of pure EPDM starts above 380 °C while in case of its nanocomposites; it takes place above 405 °C. The thermal stability of EL3 is about 40 °C higher than pure EPDM when 10% weight loss was selected as a point of comparison. This is due to the exfoliated LDH nanolayer, which in turn, obstructs the internal diffusion of heat and gaseous small molecules formed during thermal oxidation [18, 19]. For higher LDH loading, the thermal stability of the nanocomposites decreases possibly due to the presence of LDH aggregates in the EPDM matrix. It is also observed that the EPDM/LDH nanocomposites in our case shows relatively higher thermal stability compared to earlier reported EPDM/16Me-MMT nanocomposites [13] when 10% weight loss was selected as a point of comparison and may be attributed to the more homogeneous distribution of LDH nanoparticles in EPDM matrix.

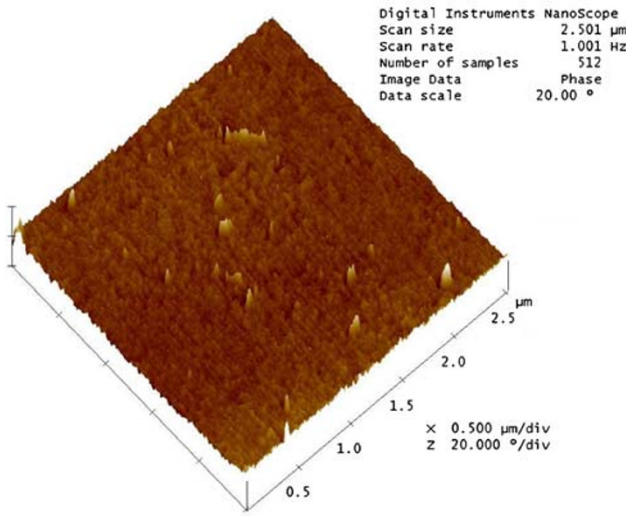

Fig. 6 Tapping mode AFM phase images of EPDM/DS-LDH nanocomposite

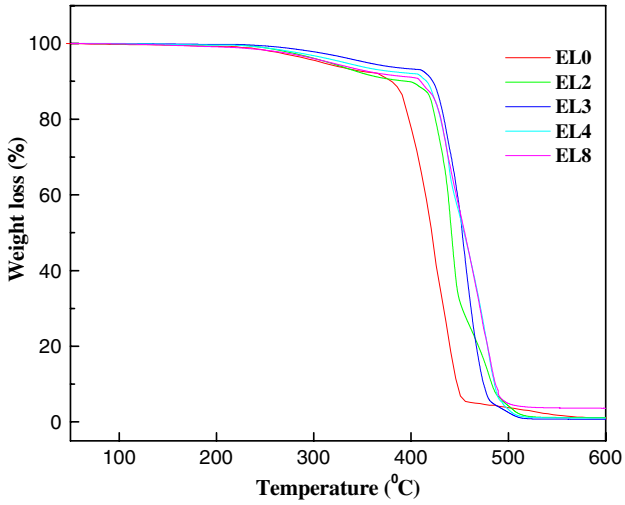

Fig. 7 TGA profiles for pure EPDM and nanocomposites with various DS-LDH contents

Conclusions

The EPDM/MgAl-LDH nanocomposites were successfully prepared by a solution blending route using dodecyl sulfate modified LDH in toluene. XRD patterns led to conclude that the exfoliated DS-LDH layers are randomly dispersed in the EPDM matrix. TEM of the nanocomposites exhibit the average thickness 2–4 nm and length 50–100 nm of the LDH particles. The AFM images of the nanocomposites exhibit the sufficient intrinsic contrast between the inorganic LDH particles and the EPDM matrix.

Thermal decomposition temperature of the nanocomposite containing 3 wt% of LDH increases more than 40 °C indicating higher thermal stability.

Acknowledgments The authors are grateful to Ministry of Human Research and Development (MHRD), India for the financial support.

References

1. F. Cavani, F. Trifiro', A. Vaccari, Catal. Today **11**, 197 (1991)
2. V. Rives (ed.), Layered double hydroxides: present and future. (Nova science publishers, 2001)
3. F. Leroux, J. P. Besse, Chem. Mater. **13**, 3507 (2001)
4. S.P. Newman, W. Jones, New. J. Chem. **22**, 105 (1998)
5. P. Meneghetti, S. Qutubuddin, Thermochim. Acta **442**, 74 (2006)
6. G.A. Wang, C.C. Wang, C.Y. Chen, Polymer **46**, 5065 (2005)
7. S.K. Srivastava, M. Pramanik, H. Acharya, J. Polym. Sci. Part B: Polym. Phys. **44**, 471 (2006)
8. D. Wang, C.A. Wilkie, J. Vinyl Additive Technol. **8**, 238 (2004)
9. M. Adachi-Pagano, C. Forano, J.P. Besse, Chem. Commun. 91 (2000)
10. S. O'Leary, D. O'Hare, G. Seeley, Chem. Commun. 1506 (2002)
11. Z.H. Liu, X.Y. Yang, Y. Makita, K. Ooi, Chem. Mater. **14**, 4800 (2002)
12. A. Usuki, A. Tukigase, M. Kato, Polymer **43**, 2185 (2002)
13. H. Acharya, M. Pramanik, S.K. Srivastava, A.K. Bhowmick, J. Appl. Polym. Sci. **93**, 2429 (2004)
14. K. Chibwe, W. Jones, Chem. Commun. 926 (1989)
15. S. Sundell, Acta. Chem. Scand. A **31**, 799 (1977)
16. O.C. Wilson, T. Olorunyolemi, A. Jaworski, L. Borum, D. Young, A. Siriwat, E. Dickens, C. Oriakhi, M. Lerner, Appl Clay Sci **15**, 265 (1999)
17. F.R. Costa, M. Abdel-Goad, U. Wagenknecht, G. Heinrich, Polymer **46**, 4447 (2005)
18. W. Chen, L. Feng, B. Qu, Chem. Mater. **16**, 368 (2004)
19. W.D. Lee, S.S. Im, H.M. Lim, K.J. Kim, Polymer **47**, 1364 (2006)